

Strong Limit on a Variable Proton-to-Electron Mass Ratio from Molecules in the Distant Universe

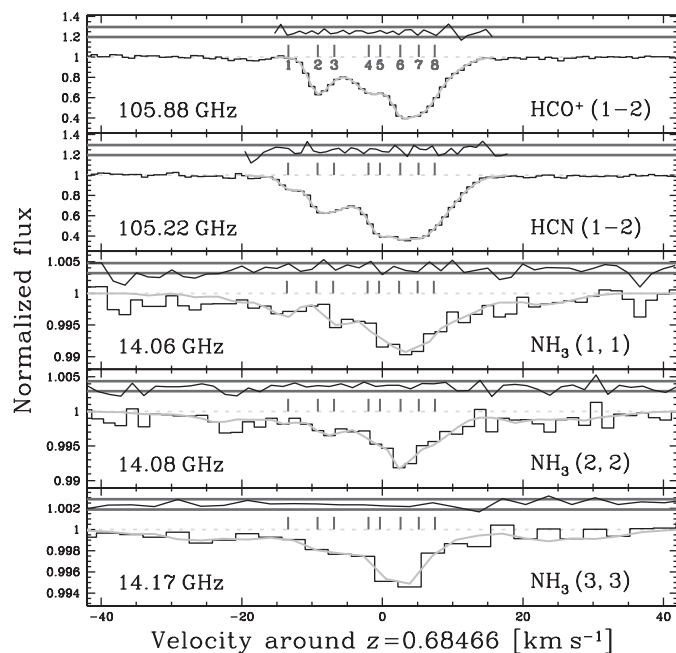
Michael T. Murphy,^{1*} Victor V. Flambaum,² Sébastien Muller,³ Christian Henkel⁴

The Standard Model of particle physics assumes that the so-called fundamental constants are universal and unchanging. Absorption lines arising in molecular clouds along quasar sightlines offer a precise test for variations in the proton-to-electron mass ratio, μ , over cosmological time and distance scales. The inversion transitions of ammonia are particularly sensitive to μ as compared to molecular rotational transitions. Comparing the available ammonia spectra observed toward the quasar B0218+357 with new, high-quality rotational spectra, we present the first detailed measurement of μ with this technique, limiting relative deviations from the laboratory value to $|\Delta\mu/\mu| < 1.8 \times 10^{-6}$ (95% confidence level) at approximately half the universe's current age—the strongest astrophysical constraint to date. Higher-quality ammonia observations will reduce both the statistical and systematic uncertainties in these observations.

The Standard Model of particle physics assumes that the fundamental constants of nature (or, at least, their low-energy limits) are the same everywhere and at every epoch in the universe. However, it cannot itself justify this assumption, nor can it predict their values. Our confidence in their constancy stems from Earth-bound laboratory experiments conducted over human time scales. Extrapolating to the entire universe seems unwise, especially considering that the physics driving the universe's accelerating expansion, labeled dark energy, is completely unknown. Nevertheless, the Earth-bound experiments achieve impressive precision: Time variations in the fine-structure constant, $\alpha \equiv e^2/\hbar c$ (where e is the electron charge, \hbar is Planck's constant h divided by 2π , and c is the speed of light), which measures the strength of electromagnetism, are limited to $\dot{\alpha}/\alpha = (-1.6 \pm 2.3) \times 10^{-17} \text{ year}^{-1}$ ($\dot{\alpha}$, α 's time derivative), whereas those in the proton-to-electron mass ratio, $\mu \equiv m_p/m_e$ (effectively, the ratio of the strong and electroweak scales) are limited to $\dot{\mu}/\mu = (-1.9 \pm 4.0) \times 10^{-16} \text{ year}^{-1}$ ($\dot{\mu}$, μ 's time derivative) (1). Still, more dramatic variations might have occurred over the 13- to 14-billion-year history of the universe, and the residual variations in our small spacetime region might remain undetectably small. It is therefore imperative to measure the constants over cosmological time and distance scales.

Variations in μ and/or α would manifest themselves as shifts in the transition energies of atoms and molecules. By comparing transition energies registered in spectra of astronomical objects with laboratory values, possible variations can, in principle, be probed over our entire observable universe and through most of its history. Because of the narrowness of the spectral features involved, absorption lines arising in gas clouds along lines of sight to background quasars are currently our most precise cosmological probes. For example, by comparing various heavy-element

Fig. 1. Spectra of the molecular transitions used in this study, registered to a heliocentric velocity scale centered on $z = 0.68466$. The nominal observed frequencies are noted in each panel. The data, normalized by fits to their continua, are plotted as black histograms. Numbered tick marks above the spectra show the positions of velocity components in our fiducial eight-component fit (the solid line following the data). The HCN and NH_3 transitions have complex hyperfine structure reflected in each velocity component; the tick marks show the position of the strongest hyperfine component in LTE (16). Residuals between the fit and data, normalized by the (constant) error array, are plotted above the spectra, bracketed by horizontal lines representing the $\pm 1\sigma$ level. The fit contains 57 free parameters: an optical depth for each component in each transition (5×8 parameters) plus a Doppler width and redshift for each component ($8 + 8$ parameters) and a single value of $\Delta\mu/\mu$. The fitted-line parameters are tabulated in (16).



¹Centre for Astrophysics and Supercomputing, Swinburne University of Technology, Mail H39, Post Office Box 218, Victoria 3122, Australia. ²School of Physics, University of New South Wales, Sydney, New South Wales 2052, Australia. ³Academia Sinica Institute of Astronomy and Astrophysics, Post Office Box 23-141, Taipei, 106 Taiwan. ⁴Max-Planck-Institut für Radioastronomie, Auf dem Hügel 69, 53121 Bonn, Germany.

*To whom correspondence should be addressed. E-mail: mmurphy@swin.edu.au

electromagnetic resonance transitions in optical quasar spectra, 5σ evidence has emerged for variations in α of ~ 5 parts in 10^6 at redshifts (z 's) $0.2 < z < 4.2$ (2–5). Although a more recent statistical sample found no variation (6), errors in the analysis prevent reliable interpretation of those results (7, 8), leaving open the possibility of a varying α .

Similarly, tentative (3σ) evidence for a fractional variation in μ of $\sim 20 \times 10^{-6}$ has recently come from two quasar spectra containing many ultraviolet (UV) H_2 transitions at $z \sim 2.8$ (9, 10). Comparison of UV heavy-element resonance lines and H α 21-cm absorption is sensitive to $\alpha^2\mu$ and, assuming α to be constant, has yielded indirect null constraints on μ variation, albeit with slightly worse precision than the direct H_2 method (11).

An alternative method for measuring μ at high redshift, suggested recently by Flambaum and Kozlov (12), is to use the sensitivity to μ variation of the ammonia inversion transitions (13) near 24 GHz. A shift in their frequencies due to a varying μ can be discerned from the cosmological redshift by comparing them to transitions with lower sensitivity to μ . Good candidates for comparison are the rotational transitions of molecules such as CO, HCO^+ , and HCN because (i) their transition frequencies depend mainly on μ and not on other fundamental quantities (such as α); (ii) they are simple molecules, commonly detected in the interstellar medium; and (iii) their rest frequencies (80 to 200 GHz) are not vastly dissimilar to the NH_3 transitions' frequencies (compared with UV and 21-cm absorption), thus

reducing possible effects due to frequency-dependent spatial structure in the background quasar's emission.

For rotational and NH₃ inversion transitions, we may write the apparent change in velocity or redshift of an absorption line due to a variation in μ as

$$\frac{\Delta v}{c} = \frac{\Delta z}{1+z} = K_i \frac{\Delta \mu}{\mu} \quad (1)$$

where K_i is the sensitivity of transition i to μ and $\Delta \mu/\mu \equiv (\mu_z - \mu_{\text{lab}})/\mu_{\text{lab}}$ for μ_{lab} and μ_z , the values of μ in the laboratory and absorption cloud at redshift z , respectively. All rotational transitions have $K_i = 1$, so comparing them with each other provides no constraint on $\Delta \mu/\mu$. However, the sensitivity of the NH₃ inversion transitions is strongly enhanced, $K_i \approx 4.46$ (12). That is, as μ varies, the NH₃ transitions shift relative to the rotational transitions.

Only one quasar absorption system displaying NH₃ absorption is currently known, that at $z = 0.68466$ toward quasar B0218+357. From z uncertainty estimates for NH₃, CO, HCO⁺, and HCN in the literature (12), the precision achievable is crudely estimated to be $\delta(\Delta \mu/\mu) \approx 2 \times 10^{-6}$. However (12), a proper measurement of $\Delta \mu/\mu$ from NH₃ would require detailed simultaneous fits to all the molecular transitions, and significantly better precision may be possible. Here we make the first detailed measurement of μ using the NH₃ inversion transitions by comparison with HCO⁺ and HCN rotational transitions.

The only published NH₃ absorption spectra are those for the $(J,K) = (1,1)$, $(2,2)$, and $(3,3)$ inversion transitions reported by (14) toward B0218+357, reproduced in Fig. 1. The channel spacing is 1.67 km s^{-1} for $(1,1)$ and $(2,2)$ and 3.3

km s^{-1} for $(3,3)$. The spectra are normalized by a low-order fit to the quasar continuum. See (14) for observational and data reduction details. The signal-to-noise ratio (SNR) for the flux is very high, ~ 1000 per channel, but because $<1\%$ of the continuum is absorbed, the effective SNR for the optical depth is quite low.

HCO⁺ and HCN(1-2) absorption toward B0218+357 was discovered more than a decade ago (15). New high-resolution ($\approx 0.9 \text{ km s}^{-1}$ per channel), high SNR (~ 100 per channel) observations of these lines were recently undertaken with the Plateau de Bure Interferometer in France (16). Figure 1 shows both spectra normalized by fits to the quasar continuum.

All spectra were registered to the heliocentric reference frame; possible errors in this procedure are discussed in (16) and shown to be negligible.

Spectra representing the 1σ uncertainty in normalized flux per channel were constructed for all the molecular spectra by calculating the root mean square (RMS) flux variations in the continuum portions of each transition. Because no large differences were observed on either side of the absorption for any transition, a simple constant-error model was adopted.

As Eq. 1 states, the signature of a varying μ would be a velocity shift between the rotational and NH₃ inversion transitions. Complicating the measurement of any shift is the velocity structure evident in Fig. 1: The profiles comprise absorption from many gas clouds, all associated with the absorbing galaxy but nevertheless moving at different velocities. The number and velocity distribution of these velocity components are unknown and must be determined from the data themselves. Each fitted velocity component is represented by a Gaussian profile parametrized by its optical depth, Doppler width,

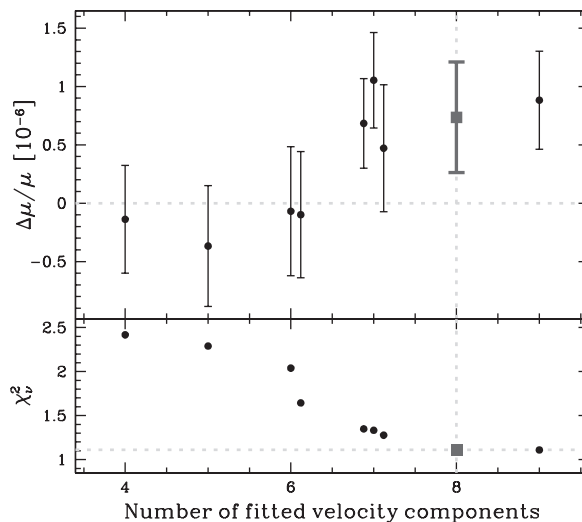
and redshift. The best-fitting parameter values are determined with a χ^2 -minimization code, VPFIT (17), designed specifically for fitting quasar absorption lines. To determine the statistically preferred velocity structure, the best-fit (that is, minimized) values of χ^2 per degree of freedom, χ^2_{ν} , are compared for several fits with different velocity structures. That with the lowest χ^2_{ν} is taken as the fiducial one (similar to an F test used to discriminate between models).

Measuring $\Delta \mu/\mu$ requires the assumption that the velocity structure is the same in all transitions. This does not mean that the ratio of optical depths of corresponding velocity components in different transitions must be constant across the profile. Rather, it means that the number and velocity distribution of components are assumed to be the same in different transitions. We discuss this assumption below, but in practice the velocity structure was determined by tying together the redshifts of corresponding velocity components in different transitions. The high-SNR rotational spectra clearly place the strongest constraints on the velocity structure, but the NH₃ spectra must be included to measure $\Delta \mu/\mu$. The Doppler widths of corresponding components were also tied together, effectively assuming a turbulent broadening mechanism.

Figure 1 shows the fiducial eight-component fit. The detailed hyperfine structure of the HCN(1-2) and NH₃ transitions is reflected in each velocity component. The relative hyperfine-level populations were fixed by assuming local thermodynamic equilibrium (LTE). The laboratory data used in the fits are tabulated in (16). Given this fit, determining $\Delta \mu/\mu$ is straightforward: A single additional free parameter is introduced for the entire absorption system, which shifts all the velocity components of each transition according to its K coefficient (Eq. 1). All parameters in the fit, including the single value of $\Delta \mu/\mu$, are varied by VPFIT to minimize χ^2 . The best-fit value is $\Delta \mu/\mu = (+0.74 \pm 0.47) \times 10^{-6}$, corresponding to a (statistically insignificant) velocity shift between the NH₃ and rotational transitions of $0.77 \pm 0.49 \text{ km s}^{-1}$. The 1σ error quoted here, formed from the diagonal terms of the final parameter covariance matrix, derives entirely from the photon statistics of the absorption spectra. A different (though intimately related) approach to determining $\Delta \mu/\mu$ and its error is discussed in (16); it provides the same result.

Fitting too few velocity components causes large systematic errors in such analyses (8). A reliable measurement of $\Delta \mu/\mu$ can be derived only from fits replicating all of the statistically significant structure in the absorption profiles. Therefore, the fiducial velocity structure must be the statistically preferred one and may be more complicated than that preferred by the human eye, especially when many transitions are fitted simultaneously. The simplest objective method to achieve this is demonstrated in Fig. 2, which shows the decrease in χ^2 as increasingly complex velocity structures are fitted. When the fit is

Fig. 2. Variation in $\Delta \mu/\mu$ and χ^2_{ν} per degree of freedom, χ^2_{ν} , of different velocity structures characterized by the number of fitted absorption components. χ^2_{ν} is defined as $\chi^2_{\nu} \equiv \sum_j N_d [d_j - m(j)]^2 / \sigma_j^2$ for d_j , the j^{th} data value with variance σ_j^2 and model value $m(j)$. The sum is over all $N_d = 223$ data points; $\nu \equiv N_d - N_{\text{par}}$ for N_{par} free model parameters. Our fiducial eight-component ($N_{\text{par}} = 57$) result is highlighted with square points. Different components were added to or removed from the fiducial fit to form each initial velocity structure, and VPFIT was run again to minimize χ^2 by varying all free parameters; results are displayed as solid circles. Two different initial fits with six components and three fits with seven components were possible; the different results are offset in the plot for clarity in these cases. Large χ^2_{ν} values for ≤ 6 components indicate that those fits are not statistically acceptable. Of the remaining fits, the eight-component fit has the lowest χ^2_{ν} . The nine-component fit has a smaller χ^2 (because more parameters are being fitted) but a marginally higher χ^2_{ν} , indicating that it is less statistically preferred than the eight-component fit. Only statistical error bars on $\Delta \mu/\mu$ are shown; see text for discussion about systematic errors.



too simple to adequately describe the data, quite different values of $\Delta\mu/\mu$ are found. On the other hand, the nine-component overfitted case provides a value and error very similar to those of the fiducial eight-component model.

The consistency of the velocity structures in the two highest-SNR transitions, HCO^+ and $\text{HCN}(1-2)$, was tested by fitting those transitions independently. Again, different fits with different velocity structures were compared to determine the statistically preferred one. Both transitions are best fit by velocity structures similar to that in Fig. 1 (16), providing some confidence that they can meaningfully be fitted simultaneously. These independent velocity structures were applied to the NH_3 transitions, and new values of $\Delta\mu/\mu$ were derived. When fitting only $\text{HCO}^+(1-2)$ and NH_3 , $\Delta\mu/\mu = (+0.67 \pm 0.51) \times 10^{-6}$; for $\text{HCN}(1-2)$ and NH_3 , $\Delta\mu/\mu = (+0.88 \pm 0.51) \times 10^{-6}$. Neither value substantially deviates from our fiducial one. The marginal increase in the 1σ error when using a single rotational transition indicates that the NH_3 spectra limit the statistical uncertainty.

To consider potential systematic uncertainties, it is important to recall our main assumption that the velocity components constituting the absorption profiles have the same redshifts in different transitions. Although the HCO^+ and $\text{HCN}(1-2)$ velocity structures are evidently similar enough for measuring $\Delta\mu/\mu$, the NH_3 spectra have a SNR that is too low for a direct comparison. And because the observed frequencies of the NH_3 (~14-GHz) and rotational (~106-GHz) transitions are somewhat different, it is possible that, if the background source morphology is frequency-dependent, some NH_3 components might arise along slightly different sightlines from those components in the rotational profiles.

B0218+357 is a $z = 0.944$ BL Lac object (18) lensed by a nearly face-on Sa/Sab $z = 0.68$ galaxy (19) in which the absorption occurs. Two lensed images, A and B, separated by 334 milli-arc sec, straddle the lensing galaxy's center, with image B much closer to the center. An Einstein ring with diameter ~300 milli-arc sec, centered near image B, has also been identified (20). B0218+357 itself has a core-jet morphology with an unresolved [$<1 \times 1$ milli-arc sec or $<7 \times 7$ pc (21)] flat-spectrum core dominating the observed 8.4-GHz emission (22). The jet has a knotty structure extending over $\sim 10 \times 10$ milli-arc sec and, like other jets, is expected to have a steep spectrum.

Various absorption lines have been detected in the $z = 0.68466$ absorber, from H α 21 cm and OH below 2 GHz (in the rest frame) (23, 24), through six H_2CO transitions at 5 to 150 GHz (25), to H_2O at 557 GHz (26), to name but a few. Furthermore, the molecular absorption arises only toward image A (25, 27–29). The flat-spectrum core should completely dominate at high frequencies; the fact that H_2CO and H_2O absorb most of the total high-frequency continuum therefore implies that at least those transitions arise only toward the core. All the

observed molecular transitions have consistent velocity structures (though most spectra have poorer resolution and/or SNR than those studied here). Thus, the most important velocity components in all transitions evidently arise toward image A's flat-spectrum, compact core (14, 29).

Nevertheless, indirect evidence suggests that the molecular clouds do not completely cover the background source (16, 30). If the covering fraction is different for the rotational and NH_3 transitions, some velocity components may appear in one and not the other. Similar problems may arise because some HCO^+ and $\text{HCN}(1-2)$ velocity components may be optically thick (16). The spurious shifts in $\Delta\mu/\mu$ that these effects may cause are difficult to estimate in general, but in (16) we conduct several fits in which different combinations of NH_3 velocity components are removed, providing an estimate of $\pm 0.7 \times 10^{-6}$. Another potential systematic error is our assumption of LTE for the $\text{HCN}(1-2)$ and NH_3 hyperfine-structure populations. Removing $\text{HCN}(1-2)$ from the analysis barely changes the measured $\Delta\mu/\mu$. Removing different parts of the hyperfine structure from the NH_3 transitions results in maximum deviations of $\pm 0.3 \times 10^{-6}$ from our fiducial value of $\Delta\mu/\mu$ (16).

Combining these two potential systematic errors in quadrature, we obtain $\Delta\mu/\mu = (+0.74 \pm 0.47_{\text{stat}} \pm 0.76_{\text{sys}}) \times 10^{-6}$, providing no evidence for cosmological variations in μ . The NH_3 spectra currently set both the statistical (stat) and systematic (sys) errors. Although the SNR and resolution clearly directly determine the former, they also indirectly influence the latter: The velocity structure of higher-quality NH_3 spectra could be more directly compared with the rotational profiles, and limits on non-LTE hyperfine-structure anomalies could be constrained by the data themselves. That is, with improved NH_3 spectra, both the statistical and systematic error components can be improved. Nevertheless, until the NH_3 data are improved, our final result is a 2σ limit on variation in μ from this single absorber: $|\Delta\mu/\mu| < 1.8 \times 10^{-6}$. This corresponds to a shift of $<1.9 \text{ km s}^{-1}$ between the NH_3 and rotational transitions.

Our new value of $\Delta\mu/\mu$ seems inconsistent with the current tentative evidence for μ variation from H_2 absorption at $z \sim 2.8$, $\Delta\mu/\mu = (+24.4 \pm 5.9) \times 10^{-6}$ (10). However, reliable comparison is difficult because cosmological time and/or space variations in μ remain poorly constrained. Clearly, a statistical sample from both techniques, covering a wide redshift range and with detailed assessment of systematic effects, is highly desirable.

Assuming that μ varies linearly with time, our measurement corresponds to a drift of $\dot{\mu}/\mu = (-1.2 \pm 0.8_{\text{stat}} \pm 1.2_{\text{sys}}) \times 10^{-16} \text{ year}^{-1}$. However, this assumption is only a convenient means for comparison with current limits from laboratory atomic clocks, $\dot{\mu}/\mu = (-1.9 \pm 4.0) \times 10^{-16} \text{ year}^{-1}$ (1); it is not motivated by any physical (necessarily un-tested) varying- μ theory.

With so few measurements of μ distributed throughout the universe, each new measurement

is an invaluable test of the most basic—and theoretically unjustifiable—assumptions in the Standard Model: that the laws of physics are universal and unchanging. The precision demonstrated here highlights the importance of discovering many more molecular absorbers to further our knowledge of fundamental physics.

References and Notes

1. T. Rosenband *et al.*, *Science* **319**, 1808 (2008).
2. J. K. Webb, V. V. Flambaum, C. W. Churchill, M. J. Drinkwater, J. D. Barrow, *Phys. Rev. Lett.* **82**, 884 (1999).
3. M. T. Murphy *et al.*, *Mon. Not. R. Astron. Soc.* **327**, 1208 (2001).
4. M. T. Murphy, J. K. Webb, V. V. Flambaum, *Mon. Not. R. Astron. Soc.* **345**, 609 (2003).
5. M. T. Murphy *et al.*, *Lecture Notes Phys.* **648**, 131 (2004).
6. H. Chand, R. Srikanand, P. Petitjean, B. Aracil, *Astron. Astrophys.* **417**, 853 (2004).
7. M. T. Murphy, J. K. Webb, V. V. Flambaum, *Phys. Rev. Lett.* **99**, 239001 (2007).
8. M. T. Murphy, J. K. Webb, V. V. Flambaum, *Mon. Not. R. Astron. Soc.* **384**, 1053 (2008).
9. A. Ivanchik *et al.*, *Astron. Astrophys.* **440**, 45 (2005).
10. E. Reinhold *et al.*, *Phys. Rev. Lett.* **96**, 151101 (2006).
11. P. Tzanavaris, M. T. Murphy, J. K. Webb, V. V. Flambaum, S. J. Curran, *Mon. Not. R. Astron. Soc.* **374**, 634 (2007).
12. V. V. Flambaum, M. G. Kozlov, *Phys. Rev. Lett.* **98**, 240801 (2007).
13. J. van Veldhoven *et al.*, *Eur. Phys. J. D* **31**, 337 (2004).
14. C. Henkel *et al.*, *Astron. Astrophys.* **440**, 893 (2005).
15. T. Wiklind, F. Combes, *Astron. Astrophys.* **299**, 382 (1995).
16. Materials and methods are available as supporting material on Science Online.
17. VPFIT is maintained by R. F. Carswell (see www.ast.cam.ac.uk/~rfc/vpfit.html).
18. J. G. Cohen, C. R. Lawrence, R. D. Blandford, *Astrophys. J.* **583**, 67 (2003).
19. T. York, N. Jackson, I. W. A. Browne, O. Wucknitz, J. E. Skelton, *Mon. Not. R. Astron. Soc.* **357**, 124 (2005).
20. A. R. Patnaik *et al.*, *Mon. Not. R. Astron. Soc.* **261**, 435 (1993).
21. Throughout we employ a standard cosmology, with Hubble constant $H_0 = 71 \text{ km s}^{-1} \text{ Mpc}^{-1}$, and matter and dark energy densities $\Omega_m = 0.27$ and $\Omega_\Lambda = 0.73$ respectively, whereby $z = 0.68466$ corresponds to a look-back time of 6.2 billion years (about half the age of the universe), with a linear angular scale of 7.1 pc milli-arc sec $^{-1}$.
22. A. D. Biggs *et al.*, *Mon. Not. R. Astron. Soc.* **338**, 599 (2003).
23. C. L. Carilli, M. P. Rupen, B. Yanny, *Astrophys. J.* **412**, L59 (1993).
24. N. Kanekar, J. N. Chengalur, A. G. de Bruyn, D. Narasimha, *Mon. Not. R. Astron. Soc.* **345**, L7 (2003).
25. N. Jethava, C. Henkel, K. M. Menten, C. L. Carilli, M. J. Reid, *Astron. Astrophys.* **472**, 435 (2007).
26. F. Combes, T. Wiklind, *Astrophys. J.* **486**, L79 (1997).
27. K. M. Menten, M. J. Reid, *Astrophys. J.* **465**, L99 (1996).
28. C. L. Carilli *et al.*, *Phys. Rev. Lett.* **85**, 5511 (2000).
29. S. Muller, M. Guélin, F. Combes, T. Wiklind, *Astron. Astrophys.* **468**, L53 (2007).
30. T. Wiklind, F. Combes, in *Highly Redshifted Radio Lines*, C. L. Carilli, S. J. E. Radford, K. M. Menten, G. I. Langston, Eds., vol. 156 of *ASP Conference Series* [Astronomical Society of the Pacific (ASP), San Francisco, 1999], pp. 202–209.
31. M.T.M. thanks the Australian Research Council for a Queen Elizabeth II Research Fellowship (DP0877998).

Supporting Online Material

www.sciencemag.org/cgi/content/full/320/5883/1611/DC1
Materials and Methods
Figs. S1 to S3
Tables S1 and S2
References and Notes

11 February 2008; accepted 22 May 2008
10.1126/science.1165352